Japanese Journal of Applied Physics

The Japan Society of Applied Physics

BRIEF NOTE

Magneto-optical switch with amorphous silicon waveguides on magneto-optical garnet

To cite this article: Eiichi Ishida *et al* 2016 *Jpn. J. Appl. Phys.* **55** 088002

Japanese Journal of Applied Physics 55, 088002 (2016)
http://doi.org/10.7567/JJAP.55.088002

BRIEF NOTE

Magneto-optical switch with amorphous silicon waveguides on magneto-optical garnet

Eiichi Ishida[1*], Kengo Miura[1], Yuya Shoji[1,2], Tetsuya Mizumoto[1,2], Nobuhiko Nishiyama[1,2], and Shigehisa Arai[1,2]

[1]Department of Electrical and Electronic Engineering, Tokyo Institute of Technology, Meguro, Tokyo 152-8552, Japan
[2]Laboratory for Future Interdisciplinary Research of Science and Technology, Tokyo Institute of Technology, Meguro, Tokyo 152-8552, Japan

*E-mail: ishida@wave.pe.titech.ac.jp

Received April 11, 2016; accepted June 6, 2016; published online July 7, 2016

We fabricated a magneto-optical (MO) switch with a hydrogenated amorphous silicon waveguide on an MO garnet. The switch is composed of a 2 × 2 Mach–Zehnder interferometer (MZI). The switch state is controlled by an MO phase shift through a magnetic field generated by a current flowing in an electrode located on the MZI. The switching operation was successfully demonstrated with an extinction ratio of 11.7 dB at a wavelength of 1550 nm.

An optical switch is a key component for building photonic network systems such as optical cross connect (OXC) and reconfigurable optical add/drop multiplexing systems, where the route of data transmission can be changed according to control signals. In these systems, densely integrated optical switches, which operate with low power consumption, are required. Optical switches with many ports have been developed with various configurations and optical effects, for example, a MEMS-based mirror switch,[1] a silica or silicon waveguide matrix switch using a thermo-optic effect,[2,3] an electro-optic effect of lithium niobate,[4] and an InP-based switch with a carrier injection[5] or quantum confined Stark effect.[6] These switches have a trade-off between the switching speed and the power consumption. Especially in the OXC systems, optical switches determine the path of optical signals and do not change the switching state frequently.[7] Therefore, a self-holding optical switch, which keeps the switching state without power supply, is attractive for reducing the power consumption of network systems.

A magneto-optical (MO) switch can have a self-holding operation by utilizing the nonvolatility of magnetic materials. In this article, we investigate an MO switch using an amorphous silicon waveguide operated by a current flow as a prototype of the self-holding switch. Among several MO materials, yttrium iron garnet $Y_3Fe_5O_{12}$ (YIG) is attractive because of its large MO effect and low optical absorption in an optical fiber communication wavelength range. By partially substituting yttrium with cerium, the MO effect is greatly enhanced.[8] A single-crystalline $CeY_2Fe_5O_{12}$ (Ce:YIG) has a saturation Faraday rotation of −4500 deg/cm at a wavelength of 1550 nm.[9] In this study, we use an MO phase shift brought about by the first order magneto-optical effect, which is proportional to the saturation Faraday rotation. The external magnetic field needed to saturate the magnetization of Ce:YIG in a film plane is ∼100 Oe. Although a single-crystalline MO garnet can be grown on a garnet substrate, the growth on other substrates is difficult. Also, an MO garnet is hardly processed into an optical waveguide. Hydrogenated amorphous silicon (a-Si:H) can be deposited at low temperatures on several platforms. We deposited a-Si:H on a single-crystalline Ce:YIG layer. Photonic circuits can be realized in small footprints owing to the strong optical confinement of the a-Si:H waveguide provided by its high refractive index.[10,11] In addition, a waveguide with a high-index core enhances the MO phase shift.[12]

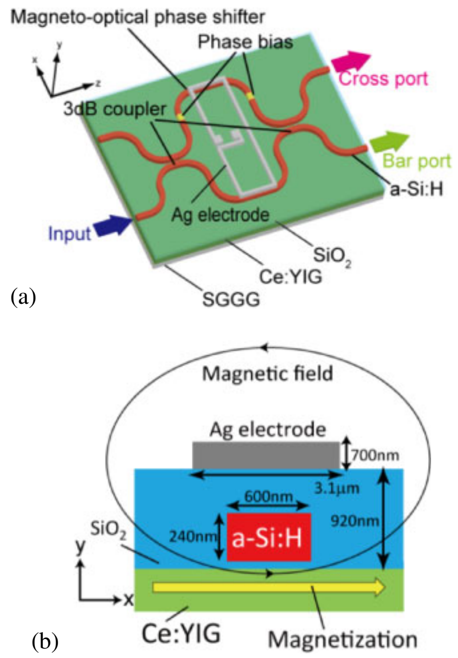

Fig. 1. (Color online) (a) Schematic of MO switch with a-Si:H waveguides. (b) Cross section of MO phase shifter.

Figure 1(a) shows a schematic illustration of the MO switch with an a-Si:H waveguide. The switch is a 2×2 Mach–Zehnder interferometer (MZI) composed of 3 dB directional couplers, an MO phase shifter, and a phase bias. The MO phase shift is induced by a magnetic field generated by the current flowing in a Ag electrode. The magnetic fields are applied to the MZI arms in antiparallel directions, outward and inward, by the current flowing in the clockwise and counterclockwise directions, respectively. The MO phase shifters provide phase differences of $-\pi/2$ and $+\pi/2$ between the MZI arms with the clockwise and counterclockwise currents, respectively. The phase bias, which is given by the optical path length difference between two arms L_{Bias}, provides a phase difference of $+\pi/2$. When the current flows in the clockwise direction, the MO phase shift is cancelled by the phase bias and the input light is transmitted to a cross port. When the current flows in the counterclockwise direction, the total phase difference amounts to π. As a result, the input light is transmitted to a bar port.

In a planar waveguide with a horizontally magnetized MO layer, the transverse magnetic (TM) mode experiences an

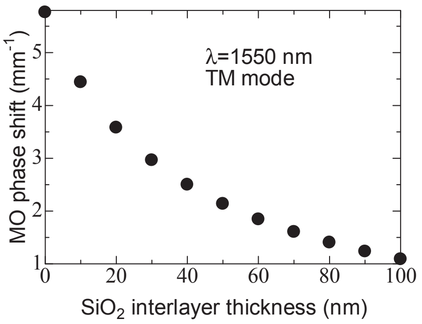

Fig. 2. MO phase shift as a function of SiO_2 interlayer thickness.

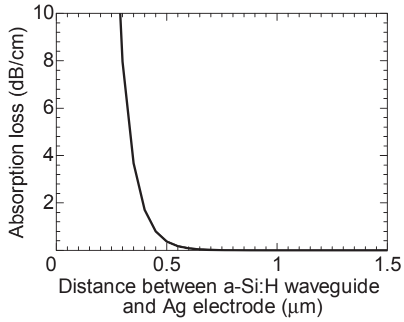

Fig. 3. Absorption loss by Ag electrode.

MO phase shift. The MO phase shift per unit propagation distance is calculated using the following equation derived from a perturbation theory.[13)]

$$\Delta\beta_{\mathrm{TM}} = \frac{2\omega\varepsilon_0}{P} \iint \mathrm{Re}(j\varepsilon_{yz}E_y^* E_z)\, dx\, dy, \tag{1}$$

where

$$P = \frac{1}{2} \iint (E \times H^* + E^* \times H)_z\, dx\, dy. \tag{2}$$

Here, E and H are the electric and magnetic fields, respectively, ω is the angular frequency, ε_0 is the vacuum permittivity, and the coordinates x, y, and z are defined in Fig. 1. The MO coefficient ε_{yz}, which is the off-diagonal component of the Ce:YIG relative permittivity tensor, is related to the saturation Faraday rotation θ_{F} and wavelength λ by $\varepsilon_{yz} = (n\lambda/\pi)\theta_{\mathrm{F}}$, when the magnetization of Ce:YIG is saturated in the x-direction. Equation (2) corresponds to the power flow along the z-direction. The MO phase shift depends on the a-Si:H core height. In this study, we used the waveguide structure shown in Fig. 1(b), where the refractive indices of a-Si:H, SiO_2, and Ce:YIG were assumed as 3.585, 1.444, and 2.20, respectively. A core height of 240 nm was chosen so as to maximize the MO phase shift. A core width of 600 nm was chosen to be a single-mode waveguide for the TM mode at a wavelength of 1550 nm.

Experimentally, we found that the propagation loss of an a-Si:H waveguide was reduced by a SiO_2 interlayer between a-Si:H and Ce:YIG. We infer that the interlayer prevents the increase in the level of Fe diffusion from Ce:YIG to a-Si:H. Figure 2 shows the MO phase shift calculated at 1550 nm as a function of SiO_2 interlayer thickness. The MO phase shift decreases exponentially as the SiO_2 interlayer thickness increases. In this design, a 30-nm-thick SiO_2 interlayer is used to ensure that no marked propagation loss is observed. The MO phase shifter length L_{MO} is calculated to be 494 μm for providing $\pm\pi/2$ magneto-optical phase differences with a magnetization saturated in the x-direction for a 30-nm-thick SiO_2 interlayer. We used $L_{\mathrm{MO}} = 1$ mm in the following fabrication to operate an MO switch with the unsaturated magnetization of Ce:YIG. Under unsaturated magnetization, the MO coefficient ε_{yz} is proportional to the x component of magnetization.

The Ag electrode used to apply a magnetic field causes optical absorption when an optical field penetrates into it. Therefore, it is necessary to determine the distance between the a-Si:H waveguide and the Ag electrode so as not to bring about a notable optical absorption while providing a sufficient magnetic field to a Ce:YIG layer. Figure 3 shows the absorption loss calculated by a finite element method as a function of the distance between the a-Si:H waveguide and the Ag electrode. In a fabricated device, we used a distance of 0.65 μm, for which the loss is <0.038 dB/cm at a wavelength of 1550 nm.

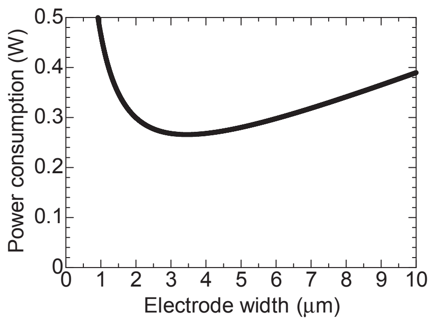

Fig. 4. Power consumption as a function of Ag electrode width.

We calculated the electric power consumption by assuming that the current density is uniform in the cross section of the Ag electrode. The resistivity and thickness of Ag were $1.59 \times 10^{-8}\,\Omega\cdot$m and 0.7 μm, respectively. The length of the electrode was 2.4 mm. Figure 4 shows the calculated electric power consumption as a function of the electrode width W under the condition that a magnetic field of 100 Oe, which is sufficient for saturating the magnetization in the film plane, is applied to the surface of Ce:YIG below the center of the a-Si:H waveguide core. It is found from this result that the power consumption becomes minimum at $W = 3.1$ μm.

The length of phase bias L_{Bias} is determined to provide a phase difference of $\pi/2 + 2m\pi$ (m: integer) by

$$L_{\mathrm{Bias}} = \frac{(m + 0.25)\lambda}{n_{\mathrm{eq}}}, \tag{3}$$

where n_{eq} denotes the equivalent refractive index. In this study, n_{eq} is 2.31 for the above designed waveguide structure at a wavelength of 1550 nm. In the following fabrication, we used $L_{\mathrm{Bias}} = 13.6$ μm for $m = 20$.

The device was fabricated by the following process. A single-crystalline Ce:YIG layer was grown on a substituted gadolinium gallium garnet (SGGG) substrate. A 30-nm-thick SiO_2 interlayer was deposited on the Ce:YIG layer by plasma-enhanced chemical vapor deposition (PCVD) with a tetraethyl-orthosilicate gas. Then, an a-Si:H layer was deposited by another PCVD with a SiH_4 gas. An a-Si:H waveguide

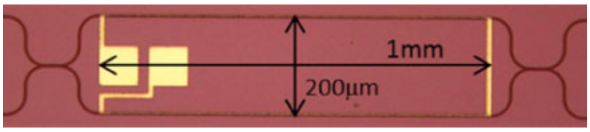

Fig. 5. (Color online) Microscopic image of fabricated MO switch.

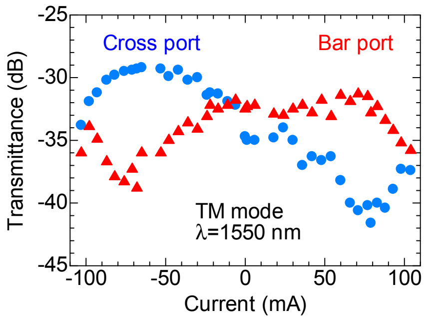

Fig. 6. (Color online) Measured transmittance of MO switch as a function of current.

was formed by electron-beam lithography followed by SF_6 reactive ion etching. Then, a SiO_2 overcladding layer was deposited. Finally, a Ag electrode was formed by the second electron-beam lithography, vacuum evaporation, and lift-off processes. Figure 5 shows a microscopic image of the fabricated device. The two arms of the MO phase shifter were separated by 200 µm, sufficient for isolating the applied magnetic field in antiparallel directions. Therefore, the aspect ratio of the MZI was larger than the schematic shown in Fig. 1(a).

During measurement, the Ag electrodes were connected to a variable voltage source to control the magnetic field applied to Ce:YIG. The TM-polarized light with a wavelength of 1550 nm was launched into the input waveguide through a lensed fiber. Figure 6 shows the transmittance measured in a fiber-device-fiber configuration, which includes the loss of the measurement setup of connectors and fiber components, and the coupling loss between the fiber and the waveguide. A positive current corresponds to the current flowing in the counterclockwise direction. In Fig. 6, painted circles and triangles represent the transmittance measured at the cross and bar ports, respectively. The transmittance was varied by changing the direction of current. This means that the switching operation was brought about by a MO effect instead of a thermo-optic effect, because the thermal effect was independent of the direction of current. When the current is −68 mA, the transmittances at the cross and bar ports were −29 and −38.5 dB, respectively. On the other hand, when the current is +71 mA, they were −40.7 and −31 dB at the cross and bar ports, respectively. As a result, the maximum extinction ratios were 11.7 and 7.5 dB at the cross and bar ports, respectively. Magnetic fields of 78 and 81 Oe are calculated to be generated with currents of 68 and 71 mA, respectively.

It is well known that the extinction ratio of MZI is greatly affected by the splitting ratios of directional couplers.[14] When two directional couplers have the same splitting ratio of 50 : 50, the extinction ratio of the bar port becomes sufficiently large for optical switching. A poor extinction ratio of 7.5 dB for the bar port of the fabricated switch is attributed to the splitting ratios of directional couplers being deviated from 50 : 50 and/or the optical losses of MZI arms being unequal. In the cross port, a sufficiently large extinction ratio is obtainable when the two directional couplers have the same splitting ratio and the losses of MZI arms are equal. An extinction ratio of 11.7 dB for the cross port indicates that this was not the case.

In conclusion, we fabricated a MO switch with an a-Si:H waveguide formed on a single-crystalline Ce:YIG layer. A switching operation based on an MO effect was successfully demonstrated by changing the current. The switch exhibited an extinction ratio of 11.7 dB in the cross port at a wavelength of 1550 nm for the TM mode.

Acknowledgments This work was supported by CREST, JST, and the Mizuho Foundation for the Promotion of Science.

1) Y. Kawajiri, N. Nemoto, T. Yamamoto, J. Yamaguchi, M. Makihara, Y. Ishii, K. Sasakura, and F. Shimokawa, 15th Microoptics Conf., 2009, p. 102.
2) S. Sohma, T. Watanabe, N. Ooba, M. Itoh, T. Shibata, and H. Takahashi, ECOC 2006, 2006, OThV4.
3) K. Suzuki, K. Tanizawa, T. Matsukawa, G. Cong, S.-H. Kim, S. Suda, M. Ohno, T. Chiba, H. Tadokoro, M. Yanagihara, Y. Igarashi, M. Masahara, S. Namiki, and H. Kawashima, Opt. Express **22**, 3887 (2014).
4) K. Suzuki, T. Yamada, O. Moriwaki, H. Takahashi, and M. Okuno, IEEE Photonics Technol. Lett. **20**, 773 (2008).
5) T. Tanemura, M. Takenaka, A. Al Amin, K. Takeda, T. Shioda, M. Sugiyama, and Y. Nakano, IEEE Photonics Technol. Lett. **20**, 1063 (2008).
6) M. Gustavsson, B. Lagerström, L. Thylén, M. Janson, L. Lundgren, A.-C. Mörner, M. Rask, and B. Stoltz, Electron. Lett. **28**, 2223 (1992).
7) K. Yonenaga, A. Takada, Y. Aoki, and S. Kinoshita, ECOC 2009, 2009, 2.5.5.
8) M. Gomi, H. Furuyama, and M. Abe, J. Appl. Phys. **70**, 7065 (1991).
9) T. Shintaku, Appl. Phys. Lett. **73**, 1946 (1998).
10) S. K. Selvaraja, E. Sleeckx, M. Schaekers, W. Bogaerts, D. V. Thourhout, P. Dumon, and R. Baets, Opt. Commun. **282**, 1767 (2009).
11) J. Kang, Y. Atsumi, M. Oda, T. Amemiya, N. Nishiyama, and S. Arai, Jpn. J. Appl. Phys. **50**, 120208 (2011).
12) H. Yokoi, T. Mizumoto, and Y. Shoji, Appl. Opt. **42**, 6605 (2003).
13) Y. Okamura, H. Inuzuka, T. Kikuchi, and S. Yamamoto, J. Lightwave Technol. **4**, 711 (1986).
14) A. Ghatak and K. Thyagarajan, *Introduction to Fiber Optics* (Cambridge University Press, Cambridge, U.K., 1998) p. 21.

